Functional Characterization of Cell-Free Expressed OprF Porin from Pseudomonas aeruginosa Stably Incorporated in Tethered Lipid Bilayers

Marco Maccarini, Landry Gayet, Jean-Pierre Alcaraz, Lavinia Liguori, Barry Stidder, Erik B. Watkins, Jean-Luc Lenormand, Donald K. Martin

LA-UR-18-26823 (Accepted Manuscript)

Functional Characterization of Cell-Free Expressed OprF Porin from Pseudomonas aeruginosa Stably Incorporated in Tethered Lipid Bilayers

Maccarini, Marco
Watkins, Erik Benjamin
Gayet, Landry
Alcaraz, Jean-Pierre
Liguori, Lavinia
Stidder, Barry
Lenormand, Jean-Luc
Martin, Donald K

To be published in: Langmuir

DOI to publisher's version: 10.1021/acs.langmuir.7b01731

LANGMUIR

Article

pubs.acs.org/Langmuir

Functional Characterization of Cell-Free Expressed OprF Porin from *Pseudomonas aeruginosa* Stably Incorporated in Tethered Lipid Bilayers

Marco Maccarini,[†,‡] Landry Gayet,[†,‡] Jean-Pierre Alcaraz,[‡] Lavinia Liguori,[‡] Barry Stidder,[‡] Erik B. Watkins,[§] Jean-Luc Lenormand,[‡] and Donald K. Martin*[,‡]

[‡]TIMC/IMAG (UMR 5525), Université de Grenoble Alpes, Grenoble, France

[§]Los Alamos National Laboratory, Los Alamos, New Mexico 87545, United States

Supporting Information

ABSTRACT: OprF has a central role in *Pseudomonas aeruginosa* virulence and thus provides a putative target for either vaccines or antibiotic cofactors that could overcome the bacterium's natural resistance to antibiotics. Here we describe a procedure to optimize the production of highly pure and functional OprF porins that are then incorporated into a tethered lipid bilayer. This is a stable biomimetic system that provides the capability to investigate structural aspects and function of OprF using and neutron reflectometry and electrical impedance spectroscopy. The recombinant OprF produced using the optimized cell-free procedure yielded a quantity of between 0.5 to 1.0 mg/mL with a purity ranging from 85 to 91% in the proteoliposomes. The recombinant OprF is capable of binding IFN-γ and is correctly folded in the proteoliposomes. Because OprF proteins form pores the biomimetic system allowed the measurement of OprF conductance using impedance spectroscopy. The neutron reflectometry measurements showed that the OprF protein is incorporated into the lipid bilayer but with parts of the protein in both the regions above and below the lipid bilayer. Those structural aspects are coherent with the current assumed structure of a transmembrane N-terminal domain composed by eight stranded beta-barrels and a globular C-terminal domain located in the periplasm. Currently there are no crystal structures available for OprF. The experimental model system that we describe provides a basis for further fundamental studies of OprF and particularly for the ongoing biotechnological development of OprF as a target for antibacterial drugs.

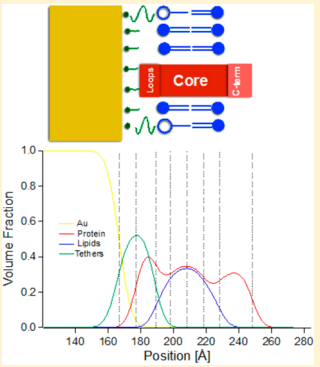

INTRODUCTION

Pseudomonas aeruginosa is a human opportunistic pathogen responsible for severe nosocomial infections of hospital patients who are difficult to treat due to the resistance of *P. aeruginosa* to most of the common antibiotics.[1] It has been hypothesized since the 1980s that the low permeability of the outer membrane of *P. aeruginosa* is responsible for such resistance to antibiotics,[2] which has been confirmed by more recent studies which showed that *P. aeruginosa* strains are resistant to most of the common antibiotics used currently in the clinic.[3−6] The outer membrane of *P. aeruginosa* contains an abundance of the protein OprF, which is a 38 kDa porin with a large diameter conducting pore. The permeability of the outer membrane is thought to be controlled by the OprF, which is the major nonspecific outer-membrane porin, but with the paradox that OprF produces a large channel that allows only a slow diffusion of various solutes.[8] That paradox is explained by the existence of an open and a closed conformer of OprF in the outer membrane of wild-type *P. aeruginosa* strains, with a relatively high proportion of OprF being the nonconducting closed conformer.[7] A proposed model for the OprF envisages a high conductance conformer in which the C-terminal of the protein is contained in the membrane, and a low conductance conformer in which the C-terminal is located in the periplasmic space. A functional fractionation technique confirmed that the open-channel conformer composed only 4.2−5.3% of the OprF population.[8] Furthermore, it is thought that the closed-channel conformer has a role in anchoring the peptidoglycan layer to the outer membrane via its C-terminus, whereas the C-terminus inserts into the outer membrane to form the open-channel conformer.[8]

OprF also has a role in the interaction with a variety of components of the host cells such as peptidoglycans for adhesion to and invasion of the cell, gamma interferon for evasion of the host immune system.[9] These interactions result in the stimulation of the expression of factors involved in the quorum-sensing dependent virulence. This includes the secretion of ExoT and ExoS toxins through the type III secretion system (T3SS) and lectin genes including LecB complex responsible for the inhibition of ciliary beating in cystic fibrosis.[10]

Recent studies have demonstrated that in addition to the role of the closed-channel conformer in the interaction with peptidoglycans, OprF may impact the biogenesis of outer

Received: May 23, 2017
Revised: August 4, 2017
Published: August 28, 2017

DOI: 10.1021/acs.langmuir.7b01731
Langmuir XXXX, XXX, XXX−XXX

membrane vesicles (OMV), which is a process known to package proteins, small molecules, and nucleic acids for delivering them to the host cells.[11,12] These vesicles are a common process used by many bacteria for communicating from cell-to-cell and for allowing the trafficking of hydrophobic signals within a bacterial population. Wessel et al.[11] recently demonstrated that inactivation of OprF results in the increase of vesicle formation and in the *P. aeruginosa* quinolone signal (PQS), which is a process known to be required for outer membrane vesicle (OMV) formation. It was demonstrated that an OprF mutant strain made by a homologous recombination resulted in a decrease of virulence of *P. aeruginosa*, in an absence of adhesion to animal cells and in the production of some virulence factors.[13] Through these pathways OprF is directly involved in biofilm formation and plays a role as a sensor of the host immune system.[14]

OprF has a central role in the biology of *P. aeruginosa* and thus provides a putative target for either vaccines or antibiotic cofactors that could overcome the bacterium's natural resistance to antibiotics. However, ongoing research is limited currently because no crystallographic structure of OprF is available and no robust OprF/biomimetic membrane system has been described for stable measurements of OprF function. Nonetheless, some insights can be gained from the molecular dynamics simulation of OprF based on the crystal structure of the homologous protein OmpA of *Escherichia coli*.[15,16] Moreover, all existing measurements of OprF have utilized a black lipid membrane formed in conjunction with hexane or pentane.[7] The lipids used to form such black lipid membranes include diphytanoylphosphatidylcholine,[17,10] oxidized cholesterol,[18,4] and egg lecithin.[4] Even though such a "solvent-free" black lipid membrane has advantages over a "painted" black lipid membrane, the surface for such membranes is only around several hundreds of micrometers in diameter and the membrane is stable for only a few hours.[19]

We have recently developed and optimized a cell-free expression system capable to overcome the problem of classical overexpression systems that cannot provide sufficient yields for functional and structural studies of highly complex membrane proteins.[20,21] This *E. coli* based cell-free expression system is capable of producing milligram amounts of functional membrane proteins of different complexities and from diverse origins. In this paper, we used our optimized cell-free expression system to obtain, in a one-step reaction, recombinant proteoliposomes containing the OprF porin in a native conformation. We then incorporated those functional OprF porins by fusing those proteoliposomes into preformed tethered lipid bilayer membranes. Such tethered lipid bilayer membranes provide a system to incorporate and study membrane proteins that is more stable than the classical black lipid bilayer.[33] We used this system to determine the low-resolution structure of the OprF conformation within the membrane using neutron reflectometry (NR). The function of the OprF incorporated into those supported lipid bilayer membranes was confirmed by measuring the channel conductance. These results provide the basis for further fundamental studies of OprF and particularly for the ongoing biotechnological development of OprF as a target for antibacterial drugs.

■ MATERIALS AND METHODS

Construction of the Prokaryotic Recombinant OprF Expression Vector. The recombinant vector pIVEX2.4-OprF with an N-terminal His Tag was constructed by cloning the PCR-amplified OprF gene from genomic DNA of *Pseudomonas aeruginosa* (forward primer, 5′-GGAATTCCATATGAAACTGAAGAACACCTTAG-3′; reverse primer 5′-GTAGAAGCTGAAGCCAAGTAACTCGAG-TAACGC-3′) into the expression vector pIVEX2.4d (Roche Diagnostics). The resulting PCR fragment was isolated, purified (QIAquick gel extraction kit, Qiagen), digested with NdeI and XhoI (Roche Diagnostics) and ligated (Rapid DNA ligation kit, Roche Diagnostics) into the digested pIVEX2.4d plasmid to obtain the pIVEX2.4-OprF recombinant plasmid, which was checked by sequencing (LGC Genomics).

Production and Purification of OprF in a Cell-Free Expression System. The expression of the full length OprF from *P. aeruginosa* was performed using a cell-free expression system[20,21] from a lysate purchased from Synthelis SAS. Briefly, the recombinant OprF membrane protein was synthesized in the presence of synthetic liposomes (liposome #1: cholesterol, 1,2-dioleoyl-*sn*-glycero-3-phosphocholine (DOPC), 1,2-dioleoyl-*sn*-glycero-3-phosphoethanolamine (DOPE), 1,2-dimyristoyl-*sn*-glycero-3-phosphate (sodium salt) molar ratio [2−4−2−2]; liposome #2: HSPC, cholesterol, DSPE-mPEG2000 molar ratio [56−39−5]; liposome #3: cholesterol, DOPC, DOPE, DOPE-mPEG2000 molar ratio [2−4−3.8−2]) directly added into the cell-free reaction mix. The plasmid pIVEX2.4-OprF and the synthetic liposomes were added at the final concentrations of 24 μg/mL and 5 mg/mL, respectively. Protein was expressed for 16 h at 25 °C and 300 rpm in a 15 mL tube for a 4 mL batch. The solution was then centrifuged at 30 000g for 20 min at 4 °C to pellet the proteoliposomes. The pellet was washed twice for 30 min at 4 °C with NaCl 5 M. The protein concentration during the different steps of the purification procedure was determined using a Coomassie gel with comparison to BSA as a standard. Analysis of the purity of OprF recombinant proteoliposomes was performed by Matrix-assisted laser desorption/ionization−time-of-flight (MALDI-TOF) mass spectroscopy (MS) after scale-up of the cell-free expression reactions and trypsin digestion of the stained bands.

Interferon-γ Binding. Binding assays of OprF proteoliposomes to INF-γ were performed using 2 protocols. In the first protocol, MaxiSorp 96-well plates (Nunc MaxiSorp, 442404) were coated for 6 h at 4 °C with INF-γ (Abcam: ab9659, 1 μg at 1 mg/mL). The second protocol was to coat MaxiSorp 96-well plates with OprF proteoliposomes. The plates coated with OprF proteoliposomes were then incubated with INF-γ (0.01 mg/mL) for 2 h at 37 °C in PBS. In those plates, the presence of bound INF-γ was detected using a mouse INF-γ primary antibody (Abcam: ab9657) and an antimouse IgG-HRP labeled antibody (GE-Healthcare: NA9310 V). The plates coated with INF-γ were incubated with OprF proteoliposomes (0.15 mg/mL) for 2 h at 37 °C in PBS. The bound OprF was revealed by using an anti-His-HRP antibody (Sigma, A7058). Protein interactions were detected after coloration using Tetramethylbenzidine (Sigma, T0440) for 10 min at room temperature and absorbance was measured at 450 nm. In separate experiments to test nonspecific binding of the antibody, BSA was used as a control to replace INF-γ.

Circular Dichroism. OprF proteoliposomes (0.5 mg/mL) were suspended in a 10 mM phosphate buffer (pH 7.4) in a Quartz Suprasyl absorption cell (0.1 cm) and the absorbance spectrum was measured at a bandwidth of 10 nm in the range between 190 and 300 nm with a scan-rate of 10 nm/min (one measurement each nanometre), using a commercial Circular Dichroism dispersion meter (Jasco, J-810). The measurements were performed at 25 °C under a flow of nitrogen (10 l/min, 1.5 bar). The blank negative control was a preparation of proteoliposomes as for the complete OprF but without DNA during production. The instrument produced a single spectrum after deconvolution and subtraction of the OprF proteoliposome and blank negative control spectra using the K2D2 model.[22]

Incorporation of recombinant OprF into tethered lipid bilayer systems. A tethered lipid bilayer membrane (tLBM) is a planar membrane composed of mobile lipids and molecules tethered to a solid planar substrate that provide a realistic model of a biomembrane. The tLBM is stable due to the chemical attachment to the substrate.[23] Moreover, the tethering molecules provide a physical

DOI: 10.1021/acs.langmuir.7b01731
Langmuir XXXX, XXX, XXX−XXX

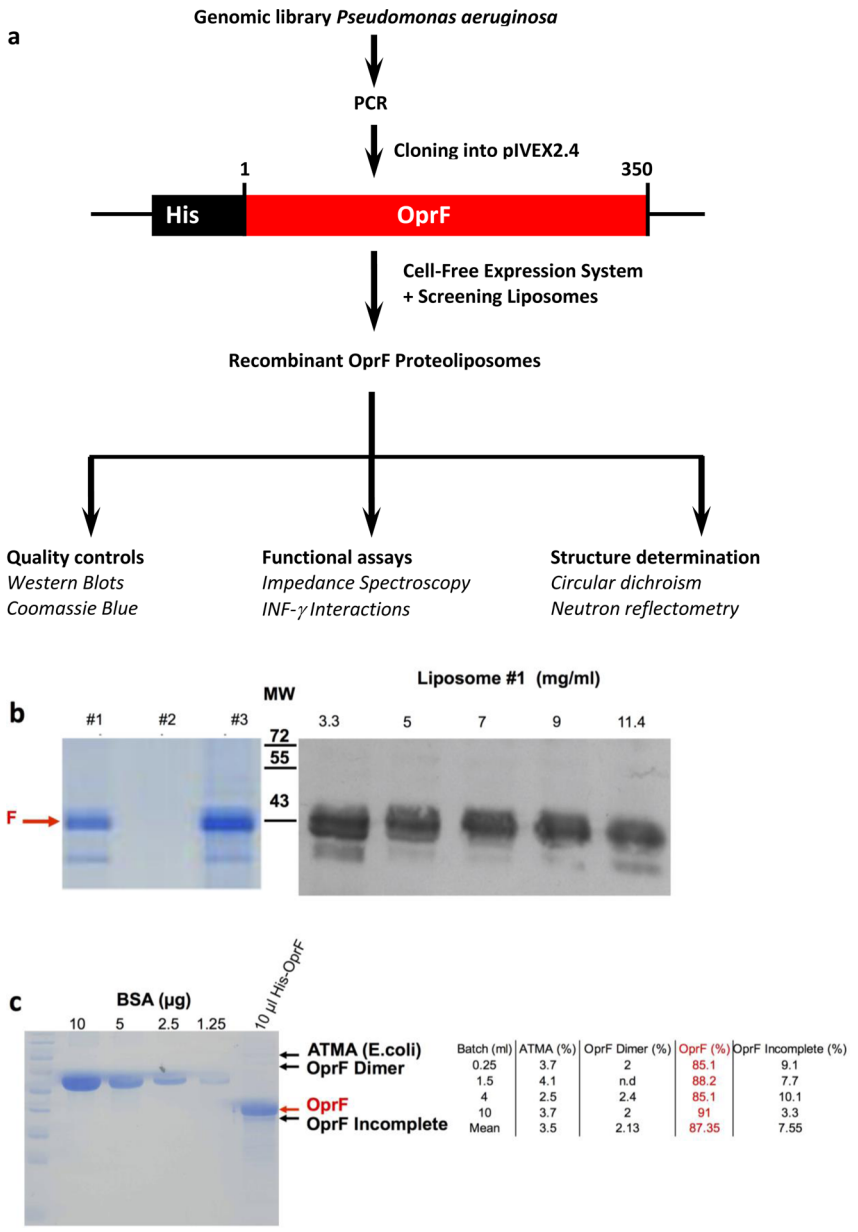

Batch (ml)	ATMA (%)	OprF Dimer (%)	OprF (%)	OprF Incomplete (%)
0.25	3.7	2	85.1	9.1
1.5	4.1	n.d	88.2	7.7
4	2.5	2.4	85.1	10.1
10	3.7	2	91	3.3
Mean	3.5	2.13	87.35	7.55

Figure 1. (a) Flow-chart of the production and characterization of the recombinant OprF protein. (b) Small-scale optimization for OprF production. The left panel shows Coomassie blue staining of OprF produced in the presence of liposomes with different lipidic composition (#1, #2, and #3). The right panel shows Western blotting (antihis antibody) of OprF synthesized in liposome #1 at different concentrations. (c) Coomassie blue staining of OprF liposomes after scale-up production and tabulated results of the MALDI-TOF-MD analysis (right panel). ATMA is an abbreviation for Mg^{2+}/Ni^{2+} transporting P-type ATPase.

separation between the bilayer and the planar substrate, which forms a hydrated reservoir space between the bilayer and the substrate. This space enables greater mechanical flexibility and fluidity to the membrane and, analogous to the intracellular space of a cell, provides a volume that may serve as a reservoir for ions involved in transport across the membrane or to accommodate transmembrane protein residues.[24]

The tLBM system[33] used was obtained by coadsorption, onto a gold-coated silicon block, of benzyl disulfide undecaethylene glycol phytanol (DLP) and benzyl disulfide tetraethylene glycol polar spacer molecules dissolved in ethanol at a concentration of 400 μM and mixed with a ratio of 10:90.[25] The surface area of the tethered lipid bilayer membrane was 2.1 mm^2 for the Electrical Impedance Spectroscopy (EIS) and around 15 cm^2 for the NR experiments. On the 2.1 mm^2 area of the EIS electrode, the tLBM was completed by using a 3 mM ethanolic solution of 30:70 (mole ratio) of glycerodiphytanylether:diphytanyletherphosphatidylcholine (AM199).

For the NR experiment, due to the large surface area (~15 cm^2) of the Si substrate (and of the significant volumes involved) a commercially available DMPC lipid was used to complete the lipid bilayer with the technique of fast solvent exchange instead of the lipid AM199 used for the impedance spectroscopy essay.

Structural Measurements Using Neutron Reflectometry. Reflectivity measurements were performed on the D17 reflectometer at the Institut Laue Langevin (Grenoble, France) in the time-of-flight mode, average resolution dQ/Q = 7%, λ range between 2 and 30 Å, with two incoming angles of 0.8 and 3.2°. The solid−liquid interface cell was oriented vertically and kept in position while changing solvents. Measurements were performed at the silicon−gold/water interface with the beam transmitted through the silicon block. The data taken at two contrasts D_2O and H_2O and were analyzed with

DOI: 10.1021/acs.langmuir.7b01731
Langmuir XXXX, XXX, XXX−XXX

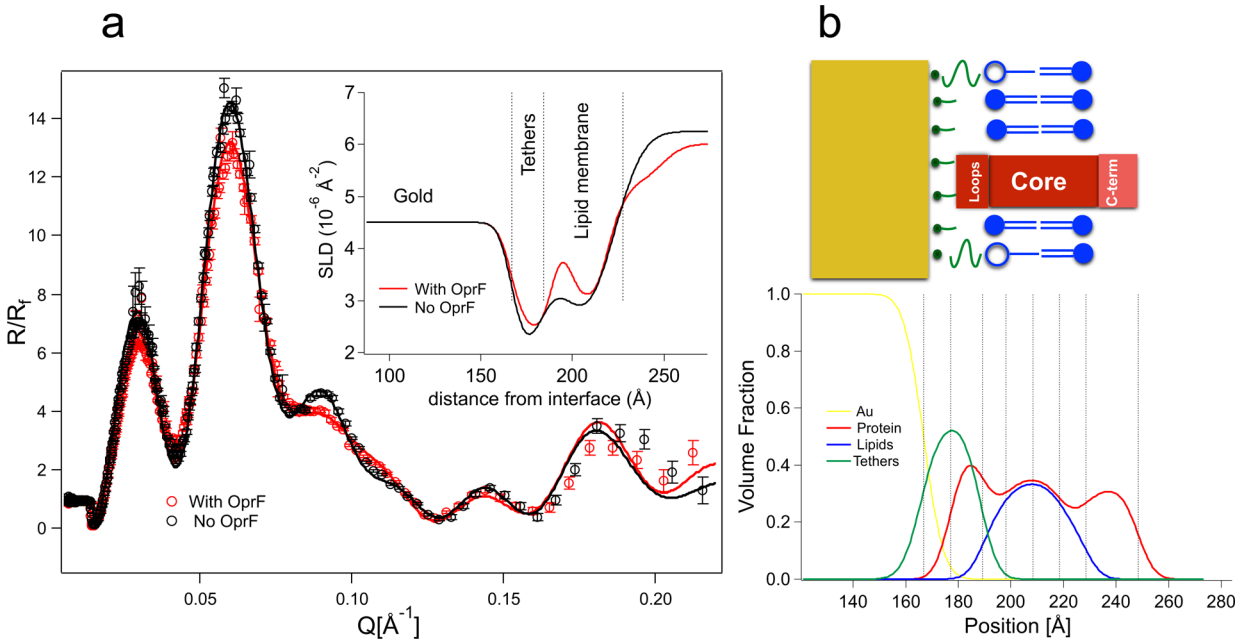

Figure 2. (a) Reflectivity profiles R/Rf (symbols) obtained for the tethered lipid bilayer system in D_2O without (black) and with (red) incorporation of the OprF. The lines correspond to the best fit to the model. In the inset, the scattering length density profiles corresponding to the D_2O contrast are shown. (b) Volume occupancy profile of the different molecular component present in the system. The blue shape with solid head corresponds to the DMPC or the AM199 free lipids. The blue shape with empty head corresponds to the part of the tethering molecule that colocalizes with the lipid bilayer. The green shapes correspond to the part of the tethering molecule that are between the lipid bilayer and the gold substrates. Details are described in ref 25.

Motofit[26] allowing simultaneous fitting of data sets from the same sample under different contrast conditions.

Conductance of OprF Using Impedance Spectrometry. Electrical Impedance Spectroscopy (EIS) applied to planar lipid bilayer membrane allows the measurement of the conductance of incorporated ion channels.[27] We performed EIS measurements on the tLBM using the TethaPod system (SDX Tethered Membranes, Australia). The TethaPod is a swept frequency ratiometric impedance spectrometer that determined the low-voltage (20 mV) AC impedance spectroscopy measurement of basal membrane conduction of the tLBM system. A sequential 20 mV excitation was applied over the frequencies 1000, 500, 200, 100, 50, 20, 10, 5, 2.5, 1.25, 0.5, 0.25, and 0.125 Hz.[28] For those measurements, recombinant OprF was incorporated into the tLBM system by the fusion of proteoliposomes (1 mg/mL). The negative control was empty liposomes produced in the same way as for the OprF proteoliposomes. The fusion of OprF proteoliposomes or empty liposomes was assisted by Dodecyl-β-D-maltoside (DDM) used at a concentration below one-fifth of its critical micellar concentration (CMC). At that low concentration, the DDM did not alter the conductance or capacitance of the tethered lipid bilayers. The recording solution for the experiments contained NaCl (140 mM) and HEPES (10 mM) at pH7.

RESULTS

Expression of Recombinant OprF. We expressed OprF using an optimized cell-free expression system in the presence of synthetic liposomes at different lipid compositions to enhance the yields and to provide an appropriate lipid environment for the OprF membrane protein (Figure 1). Compared to the other liposome preparations, the liposome composition #1 (DOPC:DOPE:DMPA:cholesterol; 4:2:2:2) used at 3.3 mg/mL provided the best yield of expressed OprF protein, with a yield ranging from 0.5 to 1.0 mg/mL (Figure 1b). Variations in liposome concentrations, sucrose, or glycerol have no influence on protein expression (Figure S1). The expression efficiencies and purities of recombinant OprF proteoliposomes were analyzed by Coomassie Blue staining (Figure 1c, left panel) and Western blotting. Scale-up production and purification resulted in highly pure recombinant OprF proteoliposomes with purity ranging from 85 to 91%. Analysis by MALDI-TOF-MS after scale-up production and in-gel trypsin digestion confirmed that the OprF membrane protein represented the main population either as in monomer or in dimer conformations (Figure 1c right panel). Circular dichroism experiments indicated that, after subtraction of the signal from empty liposomes, OprF embedded into the lipid bilayer comprised (38 ± 3)% of beta sheets and (15 ± 3)% of alpha helices (Figure S2) in accordance with the data obtained by Sugawara (40% beta sheets and 18% α helix).[8]

Structural Study of OprF Incorporated in Planar Biomimetic Membranes. We performed NR experiments in a tLBM environment in order to quantify and characterize the transfer and incorporation of OprF from the liposomes into the tLBM. These measurements provide low-resolution structural information on the lipid/protein system that confirms the incorporation of OprF into the lipid bilayer. This is important because no conclusive high-resolution crystallographic study has yet been done on this protein.

The reflectivity profiles measured on the tLBM before and after the injection of the OprF proteoliposome (D_2O contrast) are shown in Figure 2a. We performed the measurements at two contrasts by replacing the D_2O present in the measuring cell with H_2O. The complete set of measurements at the two contrasts is shown in the Supporting Information. The data in Figure 2a are displayed in terms of ratio between the reflectivity and the Fresnel reflectivity (FR) to emphasize the differences. The addition of the proteoliposomes causes significant changes in the Q range between 0.05 and 0.10 Å^{-1}.

The analysis of the NR data was obtained by simultaneous corefinement of the NR curves obtained on the system at the

DOI: 10.1021/acs.langmuir.7b01731
Langmuir XXXX, XXX, XXX−XXX

two different contrasts D_2O and H_2O. The model built to fit the reflectometry data is based on the closed conformer of the protein, which is the most probable conformation.[10] The protein spans across the lipid bilayer, which is subdivided in four layers (the head and tail regions of the two leaflets). The intramembranous core of the protein is colocalized with the lipid bilayer[29,30] and it is modeled having a cylindrical shape occupying a volume fraction φ constant across the different slabs belonging to the lipid bilayer. Furthermore, two extra slabs with part of the protein were included in the model (the C-terminus and the extra-membranous loops) at the opposite side of the lipid bilayer (Table S1). The scattering length densities (SLDs) of each term were calculated based on the atomic composition of the protein and of the of the estimated volume of the amino acid by means of the Biomolecular Scattering Length Density Calculator.[31] The effect of D-H exchange of labile hydrogen atoms was included in the calculations. In the simultaneous corefinement of the NR curves the SLD of the protein was set to that corresponding to the given contrast. The data were analyzed as follows: (i) an hypothesis on the structural properties of the system was made; (ii) the system was divided in slabs each characterized by a thickness (T), a roughness (σ); a SLD (ρ), and a volume fraction of solvent in the layer (Ψ) (Figure S3); (iii) a SLD profile was reconstructed based on the average in-plane molecular composition and structural property of each slab; (iv) the properties of each slab were optimized and refined by fitting the reflectivity obtained from the reconstructed SLD profile to the measured reflectivity.

The best-fitting model that describes the experimental reflectivity profiles after the injection of proteoliposomes in the solution indicates that the majority of the OprF protein is incorporated into the bulk of the lipid bilayer but with parts of the protein in both the regions above and below the lipid bilayer. That best-fitting model describes the closed OprF channel conformer that contains a transmembrane N-terminal domain composed by eight stranded beta-barrels and a globular C-terminal domain located in the periplasm.

To verify that the best-fitting model uniquely represents the data, we tested different structural hypotheses to build the SLD profile such as (i) no incorporation of protein; (ii) adsorption of protein on top of the bilayer; (iii) incorporation of the protein in the lipid bilayer without the extra-membranous layers. All the models based on these different hypotheses failed to properly fit the reflectivity data and resulted in significantly increased values of χ^2 (see the Supporting Information). According to our analysis it is therefore necessary to include parts of the protein into the lipid bilayer as well as at the two extra-membranous region adjacent to the bilayer to properly account of the reflectivity data. This configuration is compatible with the natural conformation hypothesized for OprF.

In Figure 2b, the SLD profiles refined from the fitting analysis are represented in terms of volume occupancy of the gold surface, the tethering molecules, the lipids and the proteins. The volume occupancies were obtained thanks to the simultaneous corefinement of the reflectivity curves at different contrasts. As a matter of fact, the change in the isotopic composition of the liquid phase helps to distinguish the scattering contributions due to the lipids and proteins from those due to the hydration molecules present in the bilayer. In Table 1, we list the optimized parameters obtained for the lipid system before and after the OprF injection. This incorporation manifests as an increase of the SLD of the tail region from

Table 1. Model Parameters Obtained for the Tethered Lipid Bilayer System in D_2O before and after the Incorporation of the OprF Protein[a]

layer	thickness (Å)	SLD ($\times 10^{-6}$Å^{-2})	solvent (%)	roughness (Å)
		before OprF		
interlayer	17 ± 2	0.6 ± 0.1	23 ± 7	8 ± 5
head inner	8 ± 2	1.2	66 ± 20	11 ± 5
tails inner	13 ± 2	−0.35	40 ± 5	11 ± 5
tails outer	13 ± 2	−0.37	40 ± 5	11 ± 5
head outer	8 ± 2	1.8	64 ± 20	11 ± 5
		after OprF		
interlayer 1	10 ± 2	0.6	34 ± 10	6 ± 5
interlayer 2	12 ± 2	2.1 (1.4) ± 0.1[b]	8 ± 10	7 ± 5
head inner	9 ± 2	2.3 (1.4) ± 0.1[b]	52 ± 20	7 ± 5
tails inner	10 ± 2	1.7 (0.9) ± 0.1[b]	31 ± 9	7 ± 5
tails outer	10 ± 2	1.7 (0.9) ± 0.1[b]	31 ± 9	7 ± 5
head outer	10 ± 2	2.7 (1.9) ± 0.1[b]	58 ± 20	7 ± 5
extra mem. layer	20 ± 5	3.5 (2.0)	77 ± 10	9 ± 5

[a]The values without error were fixed or kept to their nominal value. Note that in the layers in which the OprF is present, we list two values of SLD in view of the presence of labile hydrogen atoms that exchange with deuterium. The first value corresponds to the D_2O contrast, whereas the value in parentheses corresponds to the H_2O contrast. The extra membranous layer is due to the presence of the C-terminus that protrudes outside the membrane. [b]The error on the SLD in of the bilayer in the presence of OprF is obtained by the fitted value of the volume fraction of the protein (φ). Refer to Table S1.

approximately -0.3×10^{-6} Å^{-2} to a positive value of 0.9×10^{-6} Å^{-2} (H_2O contrast) or 1.7×10^{-6} Å^{-2} (D_2O contrast). This value is compatible with the incorporation of OprF in the membrane with a volume fraction of $\varphi = 0.56 \pm 0.03$, that can be obtained directly by the fitted value of the SLD in this region (see Table S1). Furthermore, the two extra-membranous layers on the two side of the bilayer, extend for around 12 Å in the region of the tethering molecules, and around 20 Å in the solution. The incorporation is associated with a ∼ 25% reduction of the hydration of the lipid bilayer. In order to test the dependence of the fitting results from selected parameters, we tested how the quality of the fit varied with respect to the change of the volume fraction of the incorporated protein and the thickness of the layer 7 (containing the C-term of OprF). The information can be found in Figures S7 and S8 and Tables S4 and S5.

Impedance Spectroscopy. The steady-state conductance of the tethered membrane system was measured using the Tethapod in the presence of recombinant OprF proteoliposomes and of the control (empty liposomes). The Tethapod system used an AC impedance spectroscopy technique that was adapted to the tethered lipid bilayer so as to provide a measurement of the conductance of pore-forming proteins.[33] Such impedance spectroscopy provides a sensitive measurement of the current flows across the membrane that are driven by the ion channels which were incorporated, in this case the OprF.[32] In Figure 3a, we see that the conductivity of the membrane with OprF incorporated (∼1.6 μS) is greater than the control (tLBM alone). Furthermore, the experiment shown in Figure 3b indicates that the OprF is functioning as an ion channel. The incorporation of OprF in the presence of Na ions resulted in a steady-state conductance value around 1.6 μS. The NaCl (140 mM) was replaced in a sequence of KCl (500 mM) then TrisCl (50 mM) then KCl (250 mM) and then a return to

DOI: 10.1021/acs.langmuir.7b01731
Langmuir XXXX, XXX, XXX−XXX

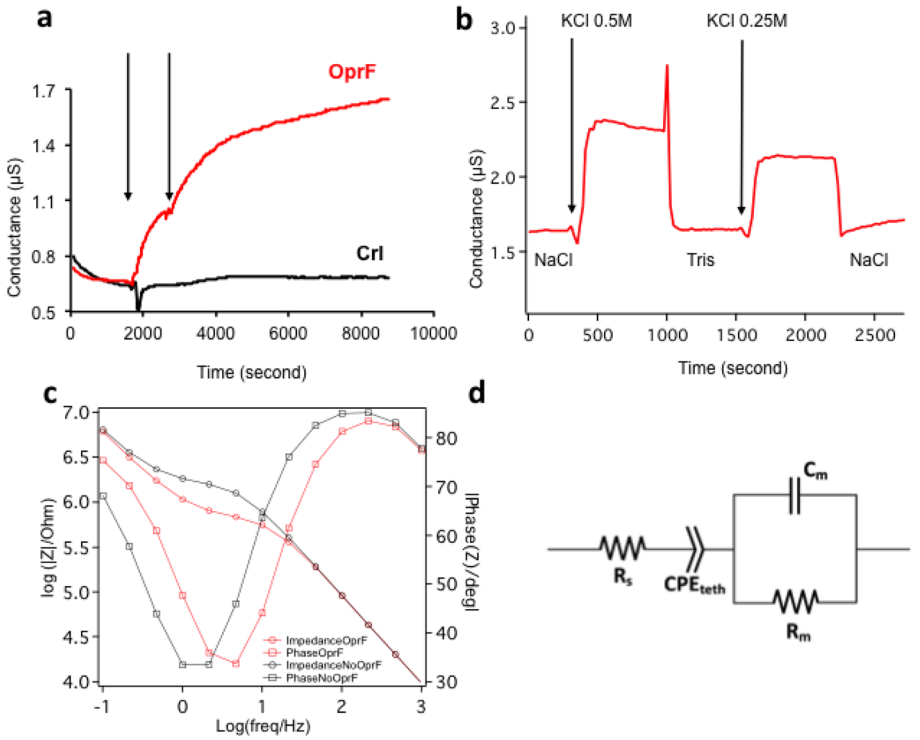

Figure 3. (a) Steady-state conductance of the tethered membrane after the insertion of OprF proteoliposomes (at the times marked with the arrows) compared to the control membrane without OprF (black curve). The arrows correspond to injections of OprF proteoliposomes. (b) Steady-state conductance of the membrane previously modified with the incorporation of OprF, when the NaCl (140 mM) is replaced by KCl (500 mM), TrisCl (50 mM) and KCl (250 mM). (c) Bode plots of the tBLM before and after the incorporation of OprF. (d) Equivalent circuit model used to analyze the EIS measurements of the tBLM, for the for the resistance of the solutions (R_s), the capacitance of the tLBM (C_m), the resistance of the membrane to account for the OprF ion channels (R_m), and a constant phase element to account for the impedance of the tether region below the tLBM (CPE_{teth}). The parameters of the fitting are provided in Table S7. The EIS measurements were also fit with an alternative analytical equivalent circuit model, with the parameters of that alternative model provided in Table S6.

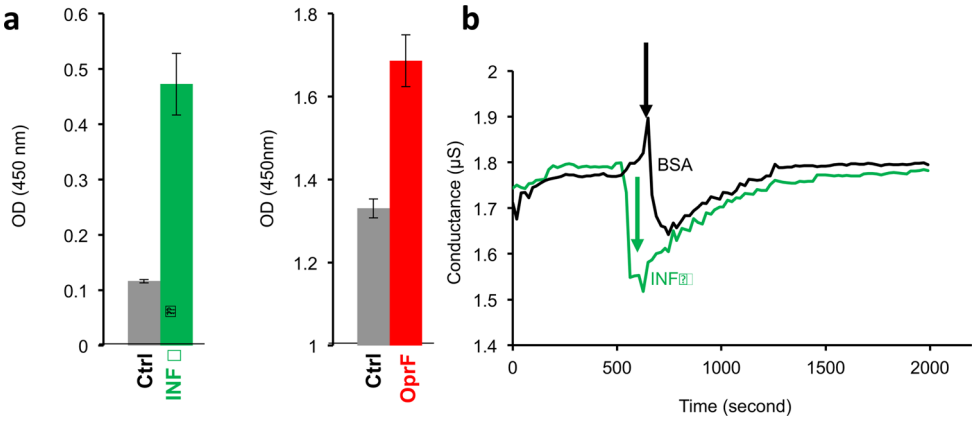

Figure 4. (a) Demonstration of the binding capacity of the recombinant OprF proteoliposomes to INF-γ using ELISA assays where IFN-γ bound to coated OprF proteoliposomes (green bar) and OprF proteoliposomes bound to coated IFN-γ (red bar). (b) Binding of INF-γ did not have a long-term effect on the conductance of OprF. There was a transient response, which was not different to the effect of BSA. (OD refers to optical density.)

NaCl (140 mM). The conductance was greatest with 500 mM (2.3 μS) compared to 250 mM (2.1 μS) of KCl. The conductance in TrisCl (~1.6 μS) was similar to that measured in NaCl (140 mM). The only concentration-dependent increase in the conductance was observed with KCl, whereas no change in the conductance was observed with NaCl and TrisCl at different concentrations.

In Figure 3c, we show the Bode plot of the tLBM before and after the incorporation of OprF. The equivalent circuit model used to fit the data is displayed in Figure 3d. This equivalent circuit model was applied previously to this tLBM.[28] The parameters of the equivalent circuit model obtained by the fitting analysis are listed in Table S7 (Supporting Information). By comparing the values obtained before and after the incorporation of the OprF we see that only the membrane resistance (R_m) is affected, with the membrane resistance reducing from ~1.5 MΩ to ~0.6 MΩ due to the permeation of ions through its pores.

To confirm the veracity of the analysis, we also used an alternative model, commonly used in the literature, based on an

DOI: 10.1021/acs.langmuir.7b01731
Langmuir XXXX, XXX, XXX−XXX

analytical description of a tethered bilayer that contains natural or artificially induced defects, such as ion channels.[33] In agreement with the previous analysis, the results from fitting the alternative model indicated that the only significant difference between before and after the incorporation of the OprF is that the resistance of the membrane reduces from ∼1.8 to ∼0.8 MΩ. The comparison between the two analyses is reported in the Figures S9 and S10 and Tables S6 and S7.

Binding Assays with Recombinant OprF Proteoliposomes. We examined the binding capacity of recombinant OprF proteoliposomes to INF-γ by ELISA assays. Those measurements of absorbance at 450 nm indicated that recombinant OprF and INF-γ directly interact (Figure 4a). The control experiment with BSA showed that there was no nonspecific binding of the antibody.

We performed impedance spectroscopy (EIS) using the TethaPod in order to measure if the binding of INF-γ interfered with the function of the OprF pore. The EIS showed that in the presence of INF-γ we observed a slight decrease in the conductance of OprF followed by a rapid return to the original conductance level (Figure 4b). However, this response was not different to the effect of BSA on the conductance of the OprF. These results indicate that the binding of INF-γ on the porin did not affect the channel function of OprF.

DISCUSSION

It has been demonstrated that OprF was capable of binding directly to the cytokine INF-γ, which is a probable molecular mechanism used by *Pseudomonas aeruginosa* to thwart the immune system activation of the host.[9] Our results confirm that the recombinant OprF we produced for the current measurements is capable of binding INF-γ, which indicates the OprF retained its biological role and was most likely oriented in a natural configuration in the proteoliposomes. Those INF-γ binding results were corroborated by circular dichroism measurements that identified that OprF was correctly folded in the proteoliposomes.

Furthermore, native OprF proteins form pores at the cytoplasmic membrane of the bacteria. The impedance spectroscopy experiments described in this article indicate that OprF protein embedded into the lipid bilayer was functional and not just simply associated with the lipid bilayer, as shown by the increase of the conductance of the tethered membrane compared to the control system.

These results are further reinforced by the low-resolution structural information obtained by NR, which revealed that a considerable amount of OprF proteins incorporated in the bilayer (∼50% of the volume) after incubation with the proteoliposomes. This is a powerful technique for the study of planar model membranes systems with a resolution of a fraction of nanometer along the normal depth direction, and has been used to elucidate nanostructural details of planar lipid membrane/protein systems.[34] By averaging along the in-plane direction, NR provides a one-dimensional structural map in terms of the SLD profiles along the direction orthogonal to the surface. From the SLD profiles the distribution of the molecular components and their volume occupancy at the interface were determined.

Using neutrons as a probe provides the advantage of "gentle" interactions with the nuclei of the atoms, thus minimizing the risk of ionizing radiation damage for delicate biological materials. At the same time, the scattering contrast can be enhanced by the use of isotope substitution. This is particularly relevant for hydrogenous materials such as lipids and protein in water because replacing hydrogen with deuterium atoms has dramatic effect on the contrast, but minimal effects on the samples. For systems immersed in liquid phases such as the biomimetic membranes studied here, changing the isotopic composition of the liquid allows the scattering contribution from the aqueous components and those coming by other interfacial component to be disentangled.

Neutron reflectometry gave a precise nanostructural characterization of the tethered bilayer system and identified differences occurring before and after the incubation with the OprF proteoliposomes. The precise modeling of the reflectivity data confirms that OprF is incorporated in the lipid bilayer in the predicted configuration. That is, the core of the protein is in the lipid bilayer with extra membranous parts above and below the lipid bilayer. Although the model is based on the most likely conformation of the incorporated OprF (the closed state conformer) with the C-terminus outside the membrane, we cannot exclude that some of the proteins are in the open conformation. In the open conformation, although the C-terminus is thought to become embedded in the intramembranous region,[10] extra-membranous loops are still present on both sides of the membrane. Furthermore, the structural information obtained by NR is averaged over a time of hours, in which the conformation of the porin fluctuates between the open and closed conformers. However, the results show that the protein is more extended on the side of the membrane pointing toward the solvent (∼20 Å) compared to the side pointing toward the substrate (∼12 Å). This might suggest a preferred orientation of the protein with the voluminous C-terminus preferentially oriented toward the solvent. For example, this orientation might be favored due to the larger space available in the direction of the solvent compared to the side closer to the substrate, where the C-terminus would compete for space with the tethered molecules. The incorporation of the OprF is linked also to a reduced hydration of the lipid bilayer, since the incorporation of the protein is accompanied by the displacement some water molecules from the lipid bilayer. In this regard it is important to note our tethered system formed by the DMPC is characterized by a low hydrated interlayer and a partially hydrated tail region. Further, it is important to note that our work demonstrates that in such conditions where the tethered bilayer presents a significant hydration of the tail region, important nanostructural information on incorporated OprF can be obtained by careful analysis of neutron reflectometry data.

CONCLUSIONS

In summary, we showed that recombinant OprF, obtained with an optimized cell-free protocol, was incorporated into tethered lipid bilayers to yield a controllable biomimetic system constructed in vitro that was measurable at the nanoscale. The several complementary techniques we utilized together provide a unified set of data for an innovative approach to investigate the function of membrane proteins. This approach was used to study the function of OprF by combining low-resolution structural data from neutron reflectometry with functional measurements of OprF in a tethered lipid membrane environment. The cell-free protocol produces OprF that folds according to the characteristics of the native porins. This experimental approach we describe provides a robust means of incorporating recombinant OprF into tethered lipid bilayer membranes, with this system stable for long periods of time.

DOI: 10.1021/acs.langmuir.7b01731
Langmuir XXXX, XXX, XXX−XXX

The system is adaptable for both large-area membranes, such as needed for structural measurements using neutron reflectometry, and for smaller-area membranes, such as needed for functional conductance measurements using electrochemical or electrophysiological measurements. These results demonstrate that the experimental model system that we describe also provides the basis for further fundamental studies of OprF and particularly for the ongoing biotechnological development of OprF as a target for antibacterial drugs.

■ ASSOCIATED CONTENT

Supporting Information

The Supporting Information is available free of charge on the ACS Publications website at DOI: 10.1021/acs.langmuir.7b01731.

Supporting materials, methods, and results (PDF)

■ AUTHOR INFORMATION

Corresponding Author

*E-mail: don.martin@univ-grenoble-alpes.fr.

ORCID

Erik B. Watkins: 0000-0001-8573-9629

Donald K. Martin: 0000-0001-5913-2372

Author Contributions

†M.M. and L.G. contributed equally and are considered co-first authors. M.M., L.G., J.L.L., and D.K.M. designed the research. L.G. and L.L. produced recombinant OprF proteoliposomes. M.M., B.S., J.P.A, E.B.W., and D.K.M. performed neutron reflectometry experiments. L.G. and J.P.A. performed electrical impedance spectroscopy experiments. L.G. performed OprF binding and circular dichroism experiments. M.M. and E.B.W. analyzed and modeled the neutron reflectometry data. M.M., L.G., J.P.A., E.B.W, J.L.L., and D.K.M. wrote the manuscript.

Notes

The authors declare no competing financial interest.

■ ACKNOWLEDGMENTS

The French government program Investissements d'Avenir (ANR-10-NANO-03-01, 2012-2016) provided financial support. We thank the NanoBio platform at UGA (Grenoble, France) for access to perform the circular dichroism measurements and the Institut Laue-Langevin for the allocation of beam time to conduct the neutron reflectometry.

■ REFERENCES

(1) Hassett, D. J.; Borchers, M. T.; Panos, R. J. Chronic obstructive pulmonary disease (COPD): evaluation from clinical, immunological and bacterial pathogenesis perspectives. *J. Microbiol.* **2014**, *52*, 211−226.

(2) Benz, R.; Hancock, R. E. W. Properties of the large ion-permeable pores formed from protein F of *Pseudomonas Aeruginosa* in lipid bilayer membranes. *Biochim. Biophys. Acta, Biomembr.* **1981**, *646*, 298−308.

(3) Morita, Y.; Tomida, J.; Kawamura, Y. Responses of *Pseudomonas aeruginosa* to antimicrobials. *Front. Microbiol.* **2014**, *4*, 422.

(4) Folkesson, A.; Jelsbak, L.; Yang, L.; Johansen, H. K.; Ciofu, O.; Høiby, N.; Molin, S. Adaptation of *Pseudomonas aeruginosa* to the cystic fibrosis airway: an evolutionary perspective. *Nat. Rev. Microbiol.* **2012**, *10*, 841−851.

(5) Sugawara, E.; Nagano, K.; Nikaido, H. Alternative folding pathways of the major porin OprF of *Pseudomonas aeruginosa*. *FEBS J.* **2012**, *279*, 910−918.

(6) Brinkman, F. S.; Bains, M.; Hancock, R. E. The amino terminus of *Pseudomonas aeruginosa* outer membrane protein OprF forms channels in lipid bilayer membranes: correlation with a three-dimensional model. *J. Bacteriol.* **2000**, *182*, 5251−5255.

(7) Angus, B. L.; Carey, A. M.; Caron, D. A.; Kropinski, A. M. B.; Hancock, R. E. W. Outer Membrane Permeability in *Pseudomonas aeruginosa*: Comparison of a Wild-type with an Antibiotic-Supersusceptible Mutant. *Antimicrob. Agents Chemother.* **1982**, *21*, 299−309.

(8) Sugawara, E.; Nestorovich, E. M.; Bezrukov, S. M.; Nikaido, H. *Pseudomonas aeruginosa* porin OprF exists in two different conformations. *J. Biol. Chem.* **2006**, *281*, 16220−16229.

(9) Wu, L.; Estrada, O.; Zaborina, O.; Bains, M.; Shen, L.; Kohler, J. E.; Patel, N.; Musch, M. W.; Chang, E. B.; Fu, Y. X.; Jacobs, M. A.; Nishimura, M. I.; Hancock, R. E.; Turner, J. R.; Alverdy, J. C. Recognition of host immune activation by *Pseudomonas aeruginosa*. *Science* **2005**, *309*, 774−777.

(10) Winstanley, C.; Fothergill, J. L. The role of quorum sensing in chronic cystic fibrosis *Pseudomonas aeruginosa* infections. *FEMS Microbiol. Lett.* **2009**, *290*, 1−9.

(11) Wessel, A. K.; Liew, J.; Kwon, T.; Marcotte, E. M.; Whiteley, M. Role of *Pseudomonas aeruginosa* peptidoglycan-associated outer membrane proteins in vesicle formation. *J. Bacteriol.* **2013**, *195*, 213−219.

(12) Ballok, A. E.; Filkins, L. M.; Bomberger, J. M.; Stanton, B. A.; O'Toole, G. A. Epoxide-mediated differential packaging of Cif and other virulence factors into outer membrane vesicles. *J. Bacteriol.* **2014**, *196*, 3633−3642.

(13) Fito-Boncompte, L.; Chapalain, A.; Bouffartigues, E.; Chaker, H.; Lesouhaitier, O.; Gicquel, G.; Bazire, A.; Madi, A.; Connil, N.; Véron, W.; Taupin, L.; Toussaint, B.; Cornelis, P.; Wei, Q.; Shioya, K.; Déziel, E.; Feuilloley, M. G.; Orange, N.; Dufour, A.; Chevalier, S. Full virulence of *Pseudomonas aeruginosa* requires OprF. *Infect. Immun.* **2011**, *79*, 1176−1186.

(14) Alhede, M.; Bjarnsholt, T.; Givskov, M.; Alhede, M. *Pseudomonas aeruginosa* biofilms: mechanisms of immune evasion. *Adv. Appl. Microbiol.* **2014**, *86*, 1−40.

(15) Straatsma, T. P.; Soares, T. A. Characterisation of the outer membrane protein OprF of *Pseudomonas aeruginosa* in a lipopolysaccharide membrane by computer simulation. *Proteins: Struct., Funct., Genet.* **2009**, *74*, 475−488.

(16) Khalid, S.; Bond, P. J.; Deol, S. S.; Sansom, M. S. Modeling and simulations of a bacterial outer membrane protein: OprF from *Pseudomonas aeruginosa*. *Proteins: Struct., Funct., Genet.* **2006**, *63*, 6−15.

(17) Rostovtseva, T. K.; Nestorovich, E. M.; Bezrukov, S. M. Partitioning of differently sized poly(ethylene glycol)s into OmpF porin. *Biophys. J.* **2002**, *82*, 160−169.

(18) Woodruff, W. A.; Parr, T. R.; Hancock, R. E. W.; Hanne, L. F.; Nicas, T. I.; Iglewski, B. H. Expression in Escherichia coli and function of *Pseudomonas aeruginosa* outer membrane porin protein F. *J. Bacteriol.* **1986**, *167*, 473−479.

(19) Brutyan, R. A.; DeMaria, C.; Harris, A. L. Horizontal 'solvent-free' lipid bimolecular membranes with two-sided access can be formed and facilitate ion channel reconstitution. *Biochim. Biophys. Acta, Biomembr.* **1995**, *1236*, 339−344.

(20) Liguori, L.; Lenormand, J. L. Production of recombinant proteoliposomes for therapeutic uses. *Methods Enzymol.* **2009**, *465*, 209−223.

(21) Liguori, L.; Stidder, B.; Alcaraz, J. P.; Lenormand, J. L.; Cinquin, P.; Martin, D. K. Cell-free production of VDAC directly into liposomes for integration with biomimetic membrane systems. *Prep. Biochem. Biotechnol.* **2016**, *46*, 546.

(22) Perez-Iratxeta, C.; Andrade-Navarro, M. A. K2D2: estimation of protein secondary structure from circular dichroism spectra. *BMC Struct. Biol.* **2008**, *8*, 25.

(23) Cranfield, C.; Carne, S.; Martinac, B.; Cornell, B. The assembly and use of tethered bilayer lipid membranes (tLBMs). In *Methods in Membrane Lipids*; Owen, D. M., Ed.; Methods in Molecular Biology; Springer: Berlin, 2015; Vol. *1232*, pp 45−5310.1007/978-1-4939-1752-5_4.

669 (24) Cornell, B. A.; Braach-Maksvytis, V. L. B.; King, L. G.; Osman,
670 P. J.; Raguse, B. L.; Wieczorek, L.; Pace, R. J. A biosensor that uses ion-
671 channel switches. *Nature* **1997**, *387*, 580−583.
672 (25) Maccarini, M.; Watkins, E. B.; Stidder, B.; Alcaraz, J.-P.; Cornell,
673 B. A.; Martin, D. K. Nanostructural determination of a lipid bilayer
674 tethered to a gold substrate. *Eur. Phys. J. E: Soft Matter Biol. Phys.* **2016**,
675 *39*, 123.
676 (26) Nelson, A. Co-refinement of multiple-contrast neutron/X-ray
677 reflectivity data using MOTOFIT. *J. Appl. Crystallogr.* **2006**, *39*, 273−
678 276.
679 (27) Korman, C. E.; Megens, M.; Ajo-Franklin, C. M.; Horsley, D. A.
680 Nanopore-spanning lipid bilayers on silicon nitride membranes that
681 seal and selectively transport ions. *Langmuir* **2013**, *29*, 4421−4425.
682 (28) Cranfield, C. G.; Cornell, B. A.; Grage, S. L.; Duckworth, P.;
683 Carne, S.; Ulrich, A. S.; Martinac, B. Transient potential gradients and
684 impedance measures of tethered bilayer lipid membranes: Pore-
685 forming peptide insertion and the effect of electroporation. *Biophys. J.*
686 **2014**, *106*, 182−189.
687 (29) Khalid, S.; Bond, P. J.; Deol, S. S.; Sansom, M. S. P. Modeling
688 and simulation of a bacterial outer membrane protein: OprF from
689 *Pseudomonas Aeruginosa* PROTEINS. *Proteins: Struct., Funct., Genet.*
690 **2006**, *63*, 6−15.
691 (30) Brinkman, F. S. L.; Bains, M.; Hancock, R. E. W. The Amino
692 Terminus of *Pseudomonas aeruginosa* Outer Membrane Protein OprF
693 Forms Channels in Lipid Bilayer Membranes: Correlation with a
694 Three-Dimensional Model. *J. Bacteriol.* **2000**, *182*, 5251.
695 (31) http://psldc.isis.rl.ac.uk/Psldc/.
696 (32) Eisenberg, R. S. Electrical Structure of Biological Cells and
697 Tissues: Impedance Spectroscopy, Stereology, And Singular Perturba-
698 tion Theory. In *Impedance Spectroscopy Theory, Experiment, and*
699 *Applications: Solid State, Corrosion, Power Sources*; Barsoukov, E.,
700 Macdonald, R., Eds.; Wiley−Interscience: New York, 2016.
701 (33) Valincius, G.; Meskauskas, T.; Ivanauskas, F. Electrochemical
702 Impedance Spectroscopy of Tethered Bilayer Membranes. *Langmuir*
703 **2012**, *28*, 977−990.
704 (34) McGillivray, D. J.; Valincius, G.; Heinrich, F.; Robertson, J. W.
705 F.; Vanderah, D. J.; Febo-Ayala, W.; Ignatjev, I.; Loesche, M.;
706 Kasianowicz, J. J. Structure of Functional *Staphylococcus aureus* a-
707 Hemolysin Channels in Tethered Bilayer Lipid Membranes. *Biophys. J.*
708 **2009**, *96*, 1547−1553.

DOI: 10.1021/acs.langmuir.7b01731
Langmuir XXXX, XXX, XXX−XXX